Reactions of bis(nitro)(α,α,α,α-tetrakis(o-pivalamidophenyl) porphinato)ferrate(III) with pyridine and imidazole. EPR and Mössbauer spectra and molecular structures of the mixed-li...

ARTICLE *in* INORGANIC CHEMISTRY · JANUARY 1991

Impact Factor: 4.76 · DOI: 10.1021/ic00007a012

Contribution from the Department of Chemistry and Biochemistry, University of Notre Dame, Notre Dame, Indiana 46556, Department of Physics, Emory University, Atlanta, Georgia 30322, and Department of Chemistry and Biochemistry, San Francisco State University, San Francisco, California 94132

Reactions of Bis(nitro)($\alpha,\alpha,\alpha,\alpha$-tetrakis(*o*-pivalamidophenyl)porphinato)ferrate(III) with Pyridine and Imidazole. EPR and Mössbauer Spectra and Molecular Structures of the Mixed-Ligand Species

Habib Nasri,[1] Yaning Wang,[2] Boi Hanh Huynh,*[,2] F. Ann Walker,*[,3] and W. Robert Scheidt*[,1]

Received September 11, 1990

The reactions of the bis(nitro)ferrate(III) picket fence porphyrin derivative [K(18-C-6)(H_2O)][Fe(NO_2)$_2$(TpivPP)] with the neutral nitrogen donors pyridine and imidazole have been examined. Both reactions yield crystalline mixed nitro–neutral nitrogen donor [Fe(NO_2)(L)(TpivPP)] species that have been characterized by UV–vis, IR, NMR, EPR, and Mössbauer spectroscopies. The EPR spectra are those of low-spin rhombic ferric porphyrinates with $g_1 = 2.98$, $g_2 = 2.37$, and $g_3 = 1.35$ (pyridine adduct) and $g_1 = 2.87$, $g_2 = 2.34$, and $g_3 = 1.56$ (imidazole adduct). Mössbauer spectra of the starting complex and the pyridine mixed-ligand product are reported. The isomer shifts are $\delta = 0.23 \pm 0.02$ and 0.25 ± 0.02 mm/s; the quadrupole splittings are $\Delta E_q = 2.01 \pm 0.03$ and 2.13 ± 0.03 mm/s, respectively, at 150 K. Mössbauer spectra have also been obtained at 4.2 K in an applied magnetic field. The magnetic spectra have been fit with a crystal field model. The crystal structure of the pyridine and imidazole adducts shows that the nitro group is in the pocket defined by the four pickets while the pyridine or imidazole is coordinated on the open face of the porphyrin. For the pyridine derivative the equatorial bonds average to 1.985 (3) Å, the axial Fe–N(NO_2) distance is 1.960 (5) Å, and the Fe–N(Py) distance is 2.093 (5) Å. Similar distances are observed in the imidazole derivative. Crystal data for the pyridine derivative: $a = 18.589$ (20) Å, $b = 19.117$ (18) Å, $c = 18.667$ (8) Å, and $\beta = 90.53$ (7)°, monoclinic, space group $C2/c$, $V = 6633$ Å^3, $Z = 4$, $FeClO_6N_{10}C_{75}H_{74}$, 5263 observed data, final data/variable = 12.3, $R_1 = 0.072$, $R_2 = 0.082$, all observations at 123 K. Crystal data for the imidazole derivative: $a = 18.318$ (5) Å, $b = 19.196$ (2) Å, $c = 18.802$ (6) Å, and $\beta = 91.72$ (1)°, monoclinic, space group C_2/c, $V = 6608$ Å^3, $Z = 4$, $FeClO_6N_{11}C_{73}H_{71}$, 3820 observed data, final data/variable = 9.8, $R_1 = 0.100$, $R_2 = 0.100$, all observations at 294 K.

Nitrite ion interacts with a number of hemoprotein derivatives with chemistry ranging from meat curing processes[4] to assimilatory[5] and dissimilatory[6] nitrite reduction. The nature of all the ligands in these species is generally not yet clear, although the assimilatory nitrite reductases seem to be unusual in at least two ways. First, these systems contain a novel isobacteriochlorin prosthetic group called siroheme,[7] and second, the heme iron appears to interact with a Fe_4S_4 cluster.[8]

We have previously reported our observations on the reactions of nitrite ion with iron(III) porphyrinates.[9,10] The reactions with iron(III) porphyrinate derivatives having open (unprotected) faces, e.g., H_2OEP or H_2TPP derivatives,[11] lead to complicated reactions in which coordinated nitrite is attacked by uncoordinated nitrite to yield, inter alia, nitrosyl derivatives.[9] The instability of the nitrite–iron(III) system with open-faced porphyrins was overcome by the use of a protected pocket derivative, i.e., picket fence porphyrin. We have previously reported[10] the preparation and structure of the bis(nitro) complex [K(18-C-6)(H_2O)][Fe(NO_2)$_2$(TpivPP)]. We report in this paper the results of the reactions of this complex with neutral nitrogen donor molecules. Such reactions proceed smoothly to replace one coordinated nitrite with the neutral nitrogen donor. We also report the characterization of these mixed-axial-ligand species and the starting bis(nitro) complex by UV–vis, electron paramagnetic resonance (EPR), and Mössbauer spectroscopies. These spectroscopic characterizations allow determinations of the "tetragonality" (Δ/λ) and "rhombicity" (V/Δ) parameters of Blumberg and Peisach[12] and provide insight into the nature of the electronic structure of the iron(III) ion for these nitro-ligated complexes. We have also carried out single-crystal structural studies of the pyridine and imidazole adducts; these structures show that the N-bound nitrite ion is located in the protected pocket, while the pyridine or imidazole ligand is coordinated to iron(III) on the open face of the porphyrin complex.

Experimental Section

General Information. UV–vis spectra were recorded on a Perkin-Elmer Lambda 4C spectrometer, and IR spectra, on a Perkin-Elmer Model 883 spectrometer (KBr pellets). EPR spectra were obtained at 77 and 5 K on a Varian E-12 EPR spectrometer operating at X-band and equipped with Varian flowing nitrogen and Air Products helium variable-temperature controllers, respectively. NMR spectra were obtained by using a Nicolet NT300 spectrometer. Both the strong- and weak-field Mössbauer spectrometers were operated in a constant-acceleration mode with a transmission arrangement, and have been described elsewhere.[13] The zero velocities of the Mössbauer spectra are referred to the centroid of the room-temperature spectrum of a metallic iron foil. A sample of [Fe(NO_2)(Py)(TpivPP)]·C_6H_5Cl for Mössbauer spectroscopy was prepared by immobilization of the crystalline material (without grinding) in paraffin wax (mp 78 °C) in a drybox. The Mössbauer spectroscopy sample of [K(18-C-6)(H_2O)][Fe(NO_2)$_2$ (TpivPP)] was handled similarly, but was also finely ground.

Preparation of [Fe(NO_2)(Py)(TpivPP)]·C_6H_5Cl. [K(18-C-6)(H_2O)][Fe(NO_2)$_2$(TpivPP)][10] (100 mg, 0.07 mmol) was dissolved in 15 mL of chlorobenzene (dried by distillation over P_2O_5), and 2 mL of pyridine (Aldrich, used without further purification) was added. The color of the solution immediately changed from deep red to light red. Single crystals of the complex were prepared by slow diffusion of dry pentane into the chlorobenzene solution. The resulting crystalline ma-

(1) University of Notre Dame.
(2) Emory University.
(3) San Francisco State University. Present address: Department of Chemistry, University of Arizona, Tucson, AZ 85721.
(4) Giddings, G. G. *J. Food Sci.* **1977**, *42*, 288. Cassens, R. G.; Greaser, M. L.; Ito, T.; Lee, M. *Food Technol.* **1979**, *33*, 46.
(5) Vegas, J. M.; Kamin, H. *J. Biol. Chem.* **1977**, *252*, 896. Coleman, K. J.; Cornish-Bowden, A.; Cole, J. A. *Biochem. J.* **1978**, *175*, 483.
(6) Firestone, M. K.; Firestone, R. B.; Tiedje, J. M. *Biochem. Biophys. Res. Commun.* **1979**, *61*, 10. Johnson, M. K.; Thomas, A. J.; Walsh, T. A.; Barber, D.; Greenwood, C. *Biochim. J.* **1980**, *189*, 285.
(7) Murphy, M. J.; Siegel, L. M.; Kamin, H. *J. Biol. Chem.* **1973**, *248*, 251. Scott, A. I.; Irwin, A. J.; Siegel, L. M. *J. Am. Chem. Soc.* **1978**, *100*, 316.
(8) Cammack, R.; Hucklesby, D.; Hewitt, E. J. *J. Biochem.* **1978**, *171*, 519. Crowe, B. A.; Patil, D. S.; Cammack, R. *Eur. J. Biochem.* **1983**, *137*, 185. Moura, I.; LeGall, J.; Lino, A. R.; Peck, H. D.; Fauque, G.; Xavier, A. V.; DerVartanian, D. V.; Moura, J. J. G.; Huynh, B. H. *J. Am. Chem. Soc.* **1988**, *110*, 1075.
(9) Finnegan, M. G.; Lappin, A. G.; Scheidt, W. R. *Inorg. Chem.* **1990**, *29*, 181.
(10) Nasri, H.; Goodwin, J. A.; Scheidt, W. R. *Inorg. Chem.* **1990**, *29*, 185.
(11) Abbreviations used in this paper: H_2OEP, octaethylporphyrin; H_2TPP, *meso*-tetraphenylporphyrin; H_2TpivPP, picket fence porphyrin; 18-C-6, 18-crown-6; Py, pyridine; HIm, imidazole; 3,5-Me_2Py, 3,5-dimethylpyridine; EPR, electron paramagnetic resonance; Mb, myoglobin.
(12) Blumberg, W. E.; Peisach, J. *Adv. Chem. Ser.* **1971**, *100*, 271.
(13) Kretchmar, S. A.; Teixeira, M.; Huynh, B. H.; Raymond, K. N. *Biol. Met.* **1988**, *1*, 26.

0020-1669/91/1330-1483$02.50/0

Table I. Crystal Data for $[Fe(NO_2)(Py)(TpivPP)]\cdot C_6H_5Cl$ and $[Fe(NO_2)(HIm)(TpivPP)]\cdot C_6H_5Cl$

formula	$FeClO_6N_{10}C_{75}H_{74}$	$FeClO_6N_{11}C_{73}H_{71}$
fw	1302.78	1289.74
temp, K	123	294
space group	$C2/c$	$C2/c$
a, Å	18.589 (20)	18.318 (5)
b, Å	19.117 (18)	19.196 (2)
c, Å	18.667 (8)	18.802 (6)
β, deg	90.53 (7)	91.72 (1)
V, Å^3	6633	6608
Z	4	4
radiation	Mo Kα	Mo Kα
criterion for observn	$F_o > 3\sigma(F_o)$	$F_o > 3\sigma(F_o)$
no. of obsd data	5260	3820
μ, mm^{-1}	0.325	0.327
R_1	0.072	0.100
R_2	0.082	0.100

terial was washed with portions of dry pentane. Typical yields are about 70%. UV-vis in C_6H_5Cl [λ_{max}, nm (log ϵ (M^{-1} cm^{-1}))]: 420 (4.05), 465 (3.18) (sh), 546 (3.06). IR [KBr pellet; $\nu(NO_2)$, cm^{-1}]: 1390 (w), 1341 (w). EPR (solid state, 77 K): $g_1 = 2.94$, $g_2 = 2.36$, $g_3 = 1.36$. NMR (^1H): H_{pyrr} ($CDCl_3$), −16.8 ppm.

Preparation of $[Fe(NO_2)(HIm)(TpivPP)]\cdot C_6H_5Cl$. An imidazole derivative can be prepared with the same procedures in comparable yields. Crystals adequate for X-ray diffraction were obtained only after the structure of the pyridine species had been determined. UV-vis in C_6H_5Cl [λ_{max}, nm (log ϵ (M^{-1} cm^{-1}))]: 421.6 (5.28), 459 (4.37) (sh), 549.6 (4.11). IR [KBr pellet; $\nu(NO_2)$, cm^{-1}]: 1303 (m), 1341 (w). EPR (C_6H_5Cl solution, 77 K): $g_1 = 2.87$, $g_2 = 2.34$, $g_3 = 1.56$. NMR (^1H): H_{pyrr} ($CDCl_3$), −16.2 ppm.

X-ray Diffraction Studies. A dark purple cyrstal of $[Fe(NO_2)(Py)(TpivPP)]\cdot C_6H_5Cl$ with approximate dimensions 0.52 × 0.33 × 0.15 mm was mounted on the end of a glass fiber. All measurements were performed with graphite-monochromated Mo Kα radiation on en Enraf-Nonius CAD4 diffractometer at 123 ± 5 K. Preliminary examination suggested a four-molecule monoclinic C-centered unit cell with the final cell constants reported in Table I. The systematic absences are consistent with either the centrosymmetric space group C_2/c (No. 13) or the noncentrosymmetric space group Cc (No. 9).

Intensity data were measured at 123 K by the θ–2θ scan method with a constant scan rate of 3°/min (in θ). Data were collected to a maximum 2θ of 54.90°. A total of 8225 $h,k,\pm l$ reflections were measured along with four standard reflections (measured every 90 min) during the course of data collection. These intensity data were reduced with the Blessing[14] profile-fitting program with corrections for Lorentz and polarization corrections but were not corrected for absorption (μ = 0.32 mm^{-1}). A total of 5263 reflections having $(\sin\theta)/\lambda < 0.576$ and $F_o \geq 3.0\sigma(F_o)$ were taken as observed. Complete crystallographic details, including data collection parameters, are given in Table SI (supplementary material).

The structure was solved in the centrosymmetric space group $C2/c$ by direct methods (MULTAN[15]). The resulting E map gave positions of most atoms; the crystallographically required 2-fold axis contains the Fe atom, the nitrogen atom of the nitro group, and the nitrogen atom and C-4 of the pyridine. After full-matrix least-squares refinement was carried to convergence, a difference Fourier map suggested possible locations for all hydrogen atoms. All hydrogen atoms were included in subsequent cycles of least-squares refinement as fixed, idealized contributors (C–H = 0.95 Å, N–H = 0.90 Å, and B(H) = 1.3B(C,N)). Final cycles of full-matrix least-squares refinement used anisotropic temperature factors for all heavy atoms. At convergence, R_1 = 0.072 and R_2 = 0.082, the error of fit was 2.26, and the final data/parameter ratio was 12.3. A final difference Fourier map was judged to be significantly free of features, with the largest peak having a height of 0.49 e/Å^3. Final atomic coordinates are listed in Table II. Anisotropic thermal parameters for all heavy atoms and the fixed hydrogen atom coordinates are available as supplementary material (Tables SII and SIII).

(14) Blessing, R. H. *Crystallogr. Rev.* **1987**, *1*, 3.
(15) Programs used in this study included local modifications of Main, Hull, Lessinger, Germain, Declerq, and Woolfson's MULTAN, Jacobson's ALLS, Zalkin's FORDAP, Busing and Levy's ORFFE, and Johnson's ORTEP2. Atomic form factors were from: Cromer, D. T.; Mann, J. B. *Acta Crystallogr., Sect. A* **1968**, *A24*, 321. Real and imaginary corrections for anomalous dispersion in the form factor of the iron atom were from: Cromer, D. T.; Liberman, D. J. *J. Chem. Phys.* **1970**, *53*, 1891. Scattering factors for hydrogen were from: Stewart, R. F.; Davidson, E. R.; Simpson, W. T. *Ibid.* **1985**, *42*, 3175. All calculations were performed on a VAX 11/730 or 3200 computer.

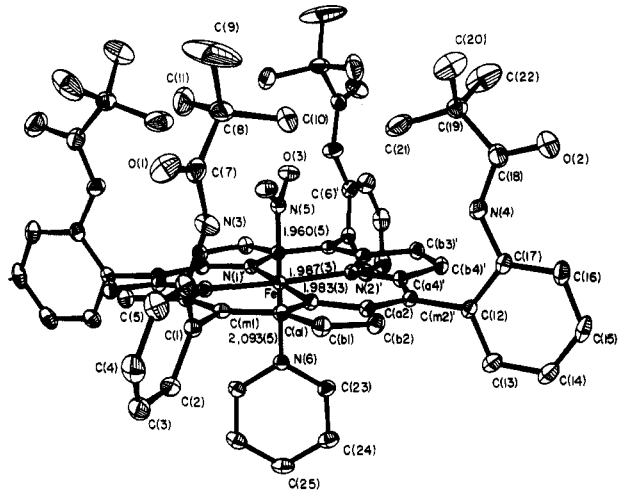

Figure 1. ORTEP diagram illustrating the molecular structure of $[Fe(NO_2)(Py)(TipvPP)]$ (30% probability ellipsoids). The labels of the crystallographically unique atoms of the molecule are shown along with the values of the bond distances in the coordination group. The nearly perpendicular orientation of the nitrite ion plane and the pyridine plane is evident.

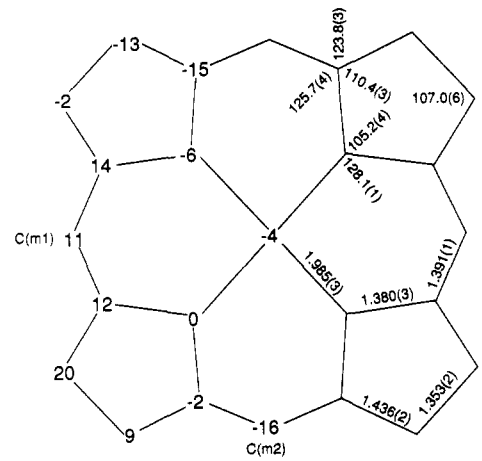

Figure 2. Formal diagram of the porphinato core of $[Fe(NO_2)(Py)(TpivPP)]$ illustrating the displacement, in units of 0.01 Å, of each unique atom from the mean plane of the 24-atom porphinato core. Negative values of displacements are toward the pyridine ligand; the 2-fold-related atoms of the core have displacement values that are equal in magnitude and sign. Also displayed on the diagram are the averaged values of each type of bond distance and angle in the porphinato core.

Crystals of the imidazole adduct were found to be isomorphous with those of the pyridine complex; unit cell parameters and data collection parameters are given in detail in Table SI. The structure of the imidazole adduct was readily solved from the porphyrin atom coordinates of the pyridine adduct. A difference Fourier map gave the coordinates of the axial ligands. The imidazole ligand has the required 2-fold axis of symmetry through the C–N bond away from the coordinated nitrogen atom. These two atoms were each refined as (N/2 + C/2) atoms; the general features of the imidazole ligand are quite reasonable. The chlorobenzene solvate was found to be seriously disordered, with two distinct orientations close to the 2-fold axis. The disorder was resolved by defining a complete chlorobenzene molecule and allowing the 2-fold symmetry to generate an overlapping second ring; each molecule was assigned an occupancy factor of 0.4. Final atomic coordinates for $[Fe(NO_2)(HIm)(TpivPP)]\cdot C_6H_5Cl$ are reported in Table III; all remaining information (tables of anisotropic thermal parameters, fixed hydrogen atoms, and values of bond distances and angles) is given as supplementary material.

Results

$[Fe(NO_2)(Py)(TpivPP)]\cdot C_6H_5Cl$ has been characterized by UV–vis, EPR, NMR, IR, and Mössbauer spectroscopies and a single-crystal X-ray structure determination. Most equivalent information has also been obtained for the imidazole adduct. The molecular structure of the $[Fe(NO_2)(Py)(TpivPP)]$ complex is illustrated in Figure 1, along with the crystallographically unique

Table II. Fractional Coordinates of $[Fe(NO_2)(Py)(TpivPP)]\cdot C_6H_5Cl$[a]

	x	y	z
Fe	1.0000	0.36094 (4)	0.2500
Cl	0.4451 (5)	0.3097 (4)	0.2020 (6)
O(1)	0.67175 (19)	0.15001 (19)	0.10810 (20)
O(2)	0.14106 (28)	0.16562 (23)	−0.07809 (23)
O(3)	1.05070 (16)	0.22608 (14)	0.27732 (16)
N(1)	0.95543 (14)	0.36211 (15)	0.15310 (14)
N(2)	0.90356 (14)	0.35853 (15)	0.29492 (14)
N(3)	0.75801 (18)	0.22924 (18)	0.13403 (22)
N(4)	1.10259 (23)	0.24806 (18)	−0.00092 (18)
N(5)	1.0000	0.25840 (21)	0.2500
N(6)	1.0000	0.47042 (21)	0.2500
C(a1)	0.88312 (17)	0.35804 (18)	0.13716 (17)
C(a2)	0.98934 (18)	0.36657 (18)	0.08784 (17)
C(a3)	0.83795 (18)	0.35254 (17)	0.26014 (18)
C(a4)	0.88715 (18)	0.35974 (19)	0.36704 (17)
C(b1)	0.87229 (19)	0.35986 (21)	0.06104 (18)
C(b2)	0.93758 (20)	0.36532 (21)	0.03040 (18)
C(b3)	0.78076 (19)	0.34828 (19)	0.31121 (19)
C(b4)	0.81085 (19)	0.35390 (20)	0.37726 (19)
C(m1)	0.82764 (18)	0.35318 (16)	0.18622 (17)
C(m2)	1.06330 (18)	0.36724 (18)	0.07717 (17)
C(1)	0.75169 (18)	0.35308 (19)	0.15832 (18)
C(2)	0.71327 (22)	0.41558 (22)	0.15930 (23)
C(3)	0.64289 (24)	0.41832 (26)	0.13442 (26)
C(4)	0.61196 (22)	0.3591 (3)	0.10641 (24)
C(5)	0.64859 (23)	0.29663 (27)	0.10533 (26)
C(6)	0.71875 (20)	0.29235 (22)	0.13227 (21)
C(7)	0.73347 (23)	0.16251 (23)	0.12458 (23)
C(8)	0.78834 (26)	0.10416 (23)	0.1366 (3)
C(9)	0.7552 (5)	0.0352 (4)	0.1149 (10)
C(10)	0.8575 (3)	0.11786 (29)	0.9718 (29)
C(11)	0.8054 (4)	0.1012 (4)	0.2180 (4)
C(12)	1.09103 (18)	0.37301 (18)	0.00228 (18)
C(13)	1.09732 (22)	0.43852 (22)	−0.03020 (22)
C(14)	1.12255 (24)	0.44457 (26)	−0.09937 (25)
C(15)	1.14211 (22)	0.38558 (29)	−0.13654 (21)
C(16)	1.13633 (23)	0.31932 (26)	−0.10563 (21)
C(17)	1.11061 (21)	0.31331 (21)	−0.03624 (19)
C(18)	1.11977 (26)	0.18209 (26)	−0.01810 (25)
C(19)	1.11150 (24)	0.12732 (21)	0.04016 (22)
C(20)	1.0609 (4)	0.0694 (3)	0.0130 (4)
C(21)	1.0813 (6)	0.1520 (3)	0.1106 (3)
C(22)	1.1852 (3)	0.0981 (4)	0.0520 (6)
C(23)	1.04051 (20)	0.50739 (20)	0.20397 (21)
C(24)	1.04177 (23)	0.57993 (22)	0.20209 (24)
C(25)	1.0000	0.61681 (29)	0.2500
C(26)	0.4696 (5)	0.3847 (6)	0.2201 (5)
C(27)	0.4492 (4)	0.4485 (6)	0.1984 (4)
C(28)	0.4783 (4)	0.5120 (6)	0.2265 (4)

[a] The estimated standard deviations of the least significant digits are given in parentheses.

bond distances around the iron atom. Equatorial bond distances (Fe–Np) average to 1.985 (3) Å,[16] and the axial Fe–N(NO_2) and Fe–N(Py) distances are 1.960 (5) and 2.093 (5) Å, respectively. A summary of coordination group parameters is given in Table IV. Averaged values of the bond distances and bond angles in the porphyrin core are shown in Figure 2. Also displayed in Figure 2 are the deviations (in units of 0.01 Å) of the crystallographically unique atoms from the mean plane of the 24-atom core. Individual values of bond distances and angles are given in Tables SIV and SV, respectively (supplementary material). These values are all consistent with a ferric low-spin complex. The angle between the nitro group plane and the pyridine plane is 77°; both ligands are perpendicular to the heme plane as required by symmetry. The nitrite ion plane makes an angle of 37° with the nearest Fe–N_p vector. Views of these ligand orientations are given in the supplementary material. Structural features for [Fe(NO_2)(HIm)(TpivPP)] are generally quite similar. An overall

(16) The numbers in parentheses following each averaged value is the estimated standard deviation calculated on the assumption that all values are drawn from the same population.

Table III. Fractional Coordinates of $[Fe(NO)_2(HIm)(TpivPP)]\cdot C_6H_5Cl$[a]

atom	x	y	z
Fe	1.0000	0.35772 (9)	0.2500
O(1)	0.6576 (4)	0.1458 (4)	0.1456 (5)
O(2)	1.1503 (6)	0.1770 (5)	−0.0733 (5)
O(3)	1.0493 (4)	0.2234 (4)	0.2757 (5)
N(1)	0.9532 (3)	0.3582 (4)	0.1541 (3)
N(2)	0.9033 (3)	0.3570 (4)	0.2927 (3)
N(3)	0.7511 (4)	0.2225 (5)	0.1372 (5)
N(4)	1.1025 (6)	0.2506 (5)	0.0010 (4)
N(5)	1.0000	0.2562 (5)	0.2500
N(6)	1.0000	0.4638 (5)	0.2500
N,C	1.0299 (5)	0.5740 (4)	0.2250 (5)
C(a1)	0.8809 (5)	0.3521 (5)	0.1372 (5)
C(a2)	0.9872 (5)	0.3643 (4)	0.0902 (5)
C(a3)	0.8371 (5)	0.3502 (5)	0.2581 (5)
C(a4)	0.8869 (5)	0.3612 (5)	0.3639 (5)
C(b1)	0.8685 (5)	0.3543 (5)	0.0617 (5)
C(b2)	0.9337 (5)	0.3630 (5)	0.0329 (4)
C(b3)	0.7792 (5)	0.3490 (5)	0.3082 (5)
C(b4)	0.8099 (5)	0.3555 (5)	0.3731 (5)
C(m1)	0.8255 (5)	0.3479 (4)	0.1845 (5)
C(m2)	1.0615 (5)	0.3679 (4)	0.0804 (5)
C(1)	0.7484 (5)	0.3481 (5)	0.1558 (5)
C(2)	0.7107 (6)	0.4110 (6)	0.1515 (6)
C(3)	0.6391 (8)	0.4137 (7)	0.1277 (7)
C(4)	0.6047 (6)	0.3559 (9)	0.1051 (7)
C(5)	0.6402 (6)	0.2898 (7)	0.1068 (6)
C(6)	0.7121 (6)	0.2861 (6)	0.1343 (6)
C(7)	0.7231 (7)	0.1569 (6)	0.1430 (6)
C(8)	0.7771 (6)	0.0986 (6)	0.1466 (7)
C(9)	0.7406 (9)	0.0349 (8)	0.1227 (14)
C(10)	0.8463 (8)	0.1156 (6)	0.1076 (8)
C(11)	0.7917 (12)	0.0815 (11)	0.2224 (9)
C(12)	1.0888 (5)	0.3747 (5)	0.0065 (5)
C(13)	1.0919 (6)	0.4369 (5)	−0.0232 (5)
C(14)	1.1164 (6)	0.4452 (6)	−0.0922 (7)
C(15)	1.1375 (6)	0.3852 (8)	−0.1299 (6)
C(16)	1.1339 (6)	0.3210 (6)	−0.0995 (6)
C(17)	1.1089 (5)	0.3160 (6)	−0.0329 (5)
C(18)	1.1226 (7)	0.1883 (7)	−0.0173 (7)
C(19)	1.1111 (8)	0.1300 (6)	0.0378 (7)
C(20)	1.0698 (13)	0.0708 (10)	0.0069 (10)
C(21)	1.0632 (16)	0.1449 (10)	0.0961 (13)
C(22)	1.1783 (9)	0.1098 (11)	0.0651 (12)
C(23)	1.0444 (5)	0.5057 (5)	0.2118 (5)

[a] The estimated standard deviations of the least significant digits are given in parentheses.

Table IV. Summary of Bond Distances (Å) and Angles (deg) in the Coordination Groups of $[Fe(NO_2)(Py)(TpivPP)]\cdot C_6H_5Cl$ and $[Fe(NO_2)(MIm)(TpivPP)]\cdot C_6H_5Cl$[a]

dist	pyridine	imidazole
Fe–N(1)	1.983 (3)	1.973 (6)
Fe–N(2)	1.987 (3)	1.967 (6)
Fe–N(5)	1.960 (5)	1.949 (10)
Fe–N(6)	2.093 (5)	2.037 (10)
N(5)–O(3)	1.233 (4)	1.191 (8)
angle	**pyridine**	**imidazole**
N(1)FeN(2)	90.8 (1)	90.0 (3)
N(1)FeN(5)	90.64 (9)	90.3 (2)
N(1)FeN(6)	89.36 (9)	89.7 (2)
N(2)FeN(5)	88.67 (9)	89.6 (2)
N(2)FeN(6)	91.33 (9)	90.4 (2)
N(5)FeN(6)	180.00	180.00
FeN(5)O(3)	120.1 (2)	121.9 (6)
O(3)N(5)O(3)′	119.9 (4)	116.1 (13)

[a] Numbers in parentheses are the estimated standard deviations in the least significant digits. Primed and unprimed symbols denote a pair of atoms related by the 2-fold axis.

view of the complex is given in Figure 3; the angle between the nitro group and the imidazole plane is 69°, and the dihedral angle between the nitrate plane and an Fe–N_p vector is again 37°. Equatorial bond distances average to 1.970 (4) Å; the axial Fe–

Table V. EPR Parameters for Low-Spin Complexes of This Study and Several Related Systems

complex	g_z	g_y	g_x	V/λ^a	Δ/λ^b	V/Δ^c	a^d	b^e	c^f	ref
$[K(18\text{-}C\text{-}6)(H_2O)][Fe(TpivPP)(NO_2)_2]$	2.67	2.49	1.57	2.55	1.91	1.34	0.963	0.205	0.172	10
$[Fe(TpivPP)(NO_2)(Py)]$	2.98	2.37	1.35	1.71	2.32	0.74	0.946	0.288	0.180	this work
$[Fe(TpivPP)(NO_2)(Im)]$	2.87	2.34	1.56	2.09	2.94	0.71	0.964	0.242	0.144	this work
$[Fe(TPP)(NCS)(Py)]$	(2.87–2.93)[g]									this work
$Mb(Fe^{III})N_3$	2.80	2.22	1.72	2.40	4.74	0.51	0.977	0.210	0.097	41
$[Fe(TPP)(CN)(Py)]$	3.31	1.76	0.34	0.66	2.07	0.32	0.824	0.483	0.231	22b
			(−0.34)[h]	0.42	1.30	0.32	0.771	0.555	0.319	
$[Fe(TPP)(C_6H_5)]$	3.54	(1.86)[i]	(0)[i]	0.53[j]	1.64[j]	0.32[j]	0.822[j]	0.538[j]	0.283[j]	42
		(1.8)[i]	(0.48)[i]	0.68[j]	2.43[j]	0.28[j]	0.856[j]	0.491[j]	0.212[j]	
		(1.7)[i]	(0.76)[i]	0.76[j]	3.53[j]	0.21[j]	0.875[j]	0.464[j]	0.157[j]	
		(1.6)[i]	(0.95)[i]	0.80[j]	5.25[j]	0.15[j]	0.888[j]	0.447[j]	0.112[j]	
		(1.5)[i]	(1.10)[i]	0.83[j]	8.74[j]	0.10[j]	0.898[j]	0.434[j]	0.071[j]	

[a] $V/\lambda = E_{yz} - E_{xz} = g_x/(g_z + g_y) + g_y(g_z - g_x)$. [b] $\Delta/\lambda = E_{xz} - E_{xy} - (1/2)V/\lambda = g_x(g_z + g_y) + g_z/(g_x - g_y) - (1/2)V/\lambda$ – tetragonality of Blumberg and Peisach.[12] [c] V/Δ = rhombicity of Blumberg and Peisach;[12] $V/\Delta \leq 2/3$ for a proper axis system.[34] [d] Orbital mixing coefficient for d_{yz}. [e] Orbital mixing coefficient for d_{xz}. [f] Orbital mixing coefficient for d_{xy}. [g] Only one weak feature observed at 5 K. [h] Alternative assignment of g_x if $g_xg_yg_z$ is negative. [i] Assumed values of g_y and g_x if $\sum g^2 = 16.0$. [j] Calculated crystal field parameters based on assumed g_x and g_y.

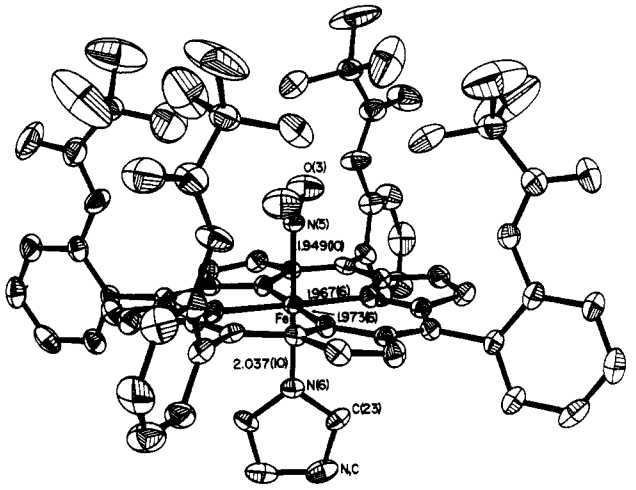

Figure 3. ORTEP diagram illustrating the molecular structure of $[Fe(NO_2)(HIm)(TpivPP)]$ and having the same relative orientation as the pyridine adduct. Only the labels of the crystallographically unique atoms of the ligands are shown; the same atom labels for the pyridine adduct otherwise apply. The values of the bond distances in the coordination group are also shown. 30% probability surfaces displayed.

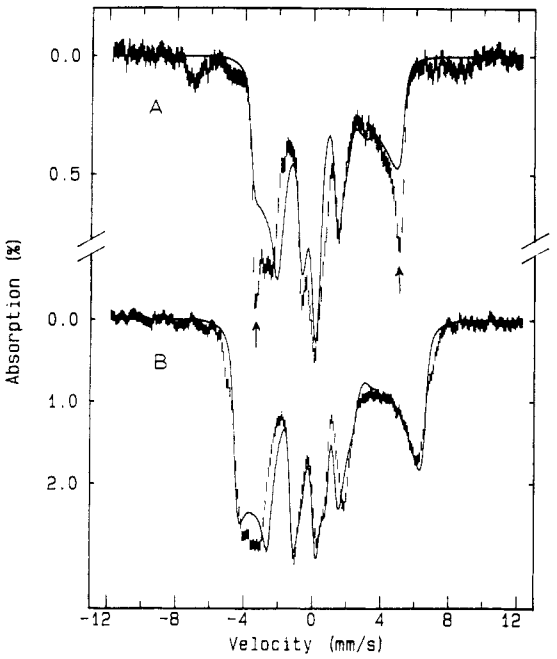

Figure 4. Mössbauer spectra of $[K(18\text{-}C\text{-}6)(H_2O)][Fe(NO_2)_2(TpivPP)]$ (A) and $[Fe(NO_2)(Py)(TpivPP)]\cdot C_6H_5Cl$ (B) derivatives recorded at 4.2 K with a magnetic field of 8 T applied parallel to the γ beam. The arrows in (A) indicate peaks originating from possible degraded sample (see text). The solid lines are theoretical simulations using the parameters listed in Table VI.

$N(NO_2)$ and Fe–N(Im) distances are 1.949 (10) and 2.037 (10) Å, respectively. Complete details are given in the supplementary material.

The EPR spectra of both the imidazole and pyridine adducts show that the complexes have low-spin states and are rhombic. However, somewhat unusual behavior was observed for the pyridine adduct, as the crystals are unstable with respect to grinding. The EPR spectrum of unground crystals of $[Fe(NO_2)(Py)(TpivPP)]$ (recorded at 77 K) is a "normal" rhombic low-spin spectrum with $g_1 = 2.98$, $g_2 = 2.37$, and $g_3 = 1.35$, but when the crystals are ground, a number of other signals also appear. This is probably the result of pyridine loss when the sample is ground.[17] Additional signals were also observed in the Mössbauer spectrum if the material was ground before measurement. Subsequently, all physical measurements were made on either lightly ground or unground crystalline material to avoid this apparent decomposition problem.

The Mössbauer spectra (150 K) of $[K(18\text{-}C\text{-}6)(H_2O)][Fe(NO_2)_2(TpivPP)]$ and the mixed-ligand species $[Fe(NO_2)(Py)(TpivPP)]\cdot C_6H_5Cl$ each exhibit similar, intense quadrupole doublets. Least-squares fits of the data yield the following parameters: quadrupole splittings $\Delta E_q = 2.01 \pm 0.03$ and 2.13 ± 0.03 mm/s and isomer shifts $\delta = 0.23 \pm 0.02$ and 0.25 ± 0.02 mm/s, for the bis(nitro) and nitro–pyridine derivatives, respectively. These parameters are characteristic of low-spin ferric heme compounds. Spectra measured at higher temperatures indicate a small temperature dependence for ΔE_q: at 190 K the ΔE_q for the bis(nitro) complex is 1.94 ± 0.03 mm/s and that for the nitro–pyridine complex is 2.10 ± 0.02 mm/s.

Figure 4 shows the 4.2 K Mössbauer spectra of $[K(18\text{-}C\text{-}6)(H_2O)][Fe(NO_2)_2(TpivPP)]$ (spectrum A) and the mixed-ligand species $[Fe(NO_2)(Py)(TpivPP)]\cdot C_6H_5Cl$ (spectrum B). The spectrum were recorded with an external field of 8 T applied parallel to the γ beam. At this temperature, low-spin ferric hemes generally exhibit Mössbauer spectra with complex magnetic patterns, as observed in Figure 4, due to the anisotropic $\tilde{g}$ and $\tilde{A}$ tensors that result from the large unquenched orbital moments of low-spin iron(III). For the sample of the bis(nitro) complex, a high-spin ferric impurity was detected. This is observed as an additional magnetic spectrum with broad absorption peaks at velocities of −7.0 and +8.6 mm/s (spectrum A). The amount of this impurity was estimated to be approximately 5%. We also noticed that the intensities of the two sharp peaks at −3.4 and +5.1 mm/s (indicated by the arrows in spectrum A) increased after the sample had been stored for a few months, suggesting that the bis(nitro) complex is unstable and slowly degrades.

(17) Similar loss of an axial pyridine ligand on sample grinding was found for $[Fe(TPP)(N_3)(Py)]$: Adams, K. M.; Rasmussen, P. G.; Scheidt, W. R.; Hatano, K. *Inorg. Chem.* **1979**, *18*, 1892.
(18) Kaduk, J. A.; Scheidt, W. R. *Inorg. Chem.* **1974**, *13*, 1875.

Discussion

Reactions of [K(18-C-6)(H_2O)][Fe(NO_2)$_2$(TpivPP)] with several neutral nitrogen donors proceed smoothly with replacement of the more exposed nitro ligand by the nitrogen donor and yield mixed-axial-ligand products. Imidazoles known to have relatively small binding constants, e.g. *N*-*R*-imidazoles,[19] appear to be in equilibrium between the mixed-ligand product and starting material as judged by product isolation and UV–vis and EPR spectra. A similar equilibrium seems to occur with the sterically hindered imidazole 2-methylimidazole. These reactions were not explored further. However, it should be noted that in all ligand replacement reactions examined, there appear to be no side reactions that lead to the conversion of coordinated nitrite to coordinated nitrosyl.

The molecular structure of [Fe(NO_2)(Py)(TpivPP)] is similar to that of other low-spin mixed-axial-ligand iron(III) porphyrinates. All such previously characterized mixed-ligand species have an anion and pyridine as the two axial ligands; the anionic ligands are cyanide,[20] N-bound thiocyanate,[21] and azide.[17] All these derivatives have a relatively long Fe–N(Py) bond distance (range 2.075–2.089 Å) and a short Fe–Ax distance (1.908–1.942 Å). The analogous 2.093 (5) and 1.960 (5) Å distances in [Fe(NO_2)(Py)(TpivPP)] follow this pattern. All these complexes have pyridine planes that are approximately oriented between an adjacent pair of Fe–N_p vectors to alleviate steric interactions; the exact angle in [Fe(NO_2)(Py)(TpivPP)] is 24°. All mixed-ligand species also have modestly D_{2d}-ruffled porphinato cores; the exact values of the displacements for [Fe(NO_2)(Py)(TpivPP)] can be found in Figure 2. One feature that is different for [Fe(NO_2)(Py)(TpivPP)] is that the small (0.04 Å) displacement of the iron atom out-of-plane is toward the pyridine ligand; in all other species the small displacement of iron is toward the anion. The axial distances can be compared with the values found in an analogous cobalt derivative, [Co(NO_2)(3,5-Me_2Py)(TPP)],[18] where the axial distances are Co–N(NO_2) = 1.948 (4) Å and Co–N(Py) = 2.036 (4) Å. The structure of the imidazole adduct is generally similar to that of the pyridine adduct; however, the equatorial and axial bond distances are all slightly shorter (see Figure 3).

The two types of axial bond distances may also be compared with values observed for analogous bisligated species. Low-spin bisligated pyridine derivatives[22] all have shorter Fe–N(Py) bonds than the 2.093 Å value found in the present case; the range of Fe–N distances is 1.995–2.031 Å. Similarly, the 2.037 Å axial Fe–N(Im) distance is longer than those observed for a series of bis(imidazole)-ligated iron(III) porphyrins.[23] The 1.960 (5) Å (or 1.949 (10) Å) Fe–N(NO_2) bond distance in the mixed pyridine (or imidazole) complexes is shorter than the 1.970 (5) and 2.001 (6) Å bond distances observed[10] in [K(18-C-6)(H_2O)][Fe(NO_2)$_2$(TpivPP)]. The shorter Fe–N(NO_2) bond distance in the mono(nitro) complexes is compatible with NO_2^- acting as a strong π acceptor with respect to a low-spin iron(III) ion.[24] Since two NO_2^- ligands with parallel relative orientations, as in [K(18-C-6)(H_2O)][Fe(NO_2)$_2$(TpivPP)], complete for the one filled metal dπ orbital, d_{xz} (vide infra), they are not able to accept as effectively as could a single ligand.

Table VI. Crystal Field and Hyperfine Parameters of [Fe(NO_2)$_2$(TpivPP)]$^-$ and [Fe(NO_2)(Py)(TpivPP)]

	[Fe(NO_2)$_2$(TpivPP)]$^-$		[Fe(NO_2)(Py)(TpivPP)]	
	theory	expt	theory	expt
Δ/λ	1.92		2.36	
V/Δ	1.33		0.74	
k	0.993		1.036	
g_x	1.57	1.57 ± 0.02	1.35	1.35 ± 0.02
g_y	2.49	2.49 ± 0.02	2.37	2.37 ± 0.02
g_z	2.67	2.67 ± 0.02	2.98	2.98 ± 0.02
$A_{xx}/g_n\beta_n$, T[a]	−11.5	−11.5	−16.7	−16.7
$A_{yy}/g_n\beta_n$, T	−3.0	−1.5 ± 2.0	2.2	6.0 ± 4.0
$A_{zz}/g_n\beta_n$, T	35.7	37.0 ± 0.5	53.0	52.0 ± 0.5
line width, mm/s		0.35		0.35
δ, mm/s[b]		0.25 ± 0.02		0.26 ± 0.02
ΔE_q, mm/s[b]		2.1 ± 0.1		2.2 ± 0.1
η		2.2 ± 0.4		1.5 ± 0.4
α,[c] deg	45	45	45	45

[a] The spectra are insensitive to this parameter, and the corresponding theoretical values are used in the simulations. [b] Experimental values at 4.2 K. [c] Angle of rotation of the principal-axis system of the $\tilde{g}$ tensor about the z axis of the cubic field.

The analysis of the 4.2 K, 8 T Mössbauer spectra used the following $S = {}^1/_2$ spin Hamiltonian:

$$\hat{\mathcal{H}} = \beta\vec{S}\cdot\tilde{g}\cdot\vec{H} + \vec{S}\cdot\tilde{A}\cdot\vec{I} + (eQV_{zz}/4)[I_z^2 - I(I+1)/3 + (\eta/3)(I_x^2 - I_y^2)] - g_n\beta_n\vec{H}\cdot\vec{I} \quad (1)$$

The g values were obtained from the EPR measurements, and the quadrupole splittings were determined from the high-temperature Mössbauer spectra. Estimates of the hyperfine coupling tensor $\tilde{A}$ were made by using the method developed by Oosterhuis and Lang,[25] who showed that the ligand-field model introduced by Griffith[26] for low-spin iron(III) could also be used to calculate the $\tilde{A}$ tensor, provided the g values and the crystal field symmetry were known.[25,27] Thus the only free parameter in eq 1 is the asymmetry parameter η. With an assumed symmetry and the g values known from EPR measurements, we can use eq 1 to simulate theoretical spectra and compare them with the experimental spectra. This method of analysis has been successfully applied in several Mössbauer investigations of low-spin ferric heme complexes.[27-30]

At first, for simplicity, we assumed rhombic symmetry for both the bis(nitro) and the mixed nitro–pyridine complexes. With rhombic symmetry, the principal-axis systems of the $\tilde{g}$ and $\tilde{A}$ tensors correspond with the cubic field axes. This assumption, however, yielded A values that are incompatible with the experimental data. Next, we assumed that the $\tilde{g}$ tensor axis system (i.e., the rhombic field axes) is rotated about the z axis of the cubic field by an angle, α, of 45°.[31] We then obtained parameters that yielded calculated spectra in agreement with the experimental data. The final sets of spin-Hamiltonian parameters were determined by varying the A values and η until the theoretical simulation best fit the experimental spectra. The parameters thus obtained are listed in Table VI, and the corresponding 8-T theoretical spectra are plotted as the solid lines in Figure 4. The agreement between the simulations and the experimental spectra is seen to be quite reasonable. These sets of parameters also yield simulations in good agreement with spectra recorded in external magnetic fields of 6, 4, and 2 T (spectra not shown).

(19) Walker, F. A.; Lo, M. W.; Ree, M. T. *J. Am. Chem. Soc.* **1976**, *98*, 5552.
(20) Scheidt, W. R.; Lee, Y. J.; Luangdilok, W.; Haller, K. J.; Anzai, K.; Hatano, K. *Inorg. Chem.* **1983**, *22*, 1516.
(21) Scheidt, W. R.; Lee, Y. L.; Geiger, D. K.; Taylor, K.; Hatano, K. *J. Am. Chem. Soc.* **1982**, *104*, 3367.
(22) (a) Scheidt, W. R.; Geiger, D. K.; Haller, K. J. *J. Am. Chem. Soc.* **1982**, *104*, 495. (b) Inniss, D.; Soltis, S. M.; Strouse, C. E. *J. Am. Chem. Soc.* **1988**, *110*, 5644. (c) Safo, M.; Scheidt, W. R. Unpublished results.
(23) (a) Countryman, R.; Collins, D. M.; Hoard, J. L. *J. Am. Chem. Soc.* **1969**, *91*, 5166. (b) Little, R. G.; Dymock, K. R.; Ibers, J. A. *J. Am. Chem. Soc.* **1975**, *97*, 4532. (c) Scheidt, W. R.; Osvath, S. R.; Lee, Y. J. *J. Am. Chem. Soc.* **1987**, *109*, 1958. (d) Quinn, R.; Valentine, J. S.; Byrn, M. P.; Strouse, C. E. *J. Am. Chem. Soc.* **1987**, *109*, 3301. (e) Scheidt, W. R.; Geiger, D. K.; Lee, Y. J.; Reed, C. A.; Lang, G. *Inorg. Chem.* **1987**, *26*, 1039. (f) Safo, M.; Scheidt, W. R. Unpublished results.
(24) The importance of π bonding for the nitrite ion with iron porphyrinates is given by the observation that a *single* nitrite ion leads to a low-spin iron(II) porphyrinate. A strong π-acceptor ligand is thus indicated: Nasri, H.; Wang, Y.; Huynh, B. H.; Scheidt, W. R.; *J. Am. Chem. Soc.* **1991**, *113*, 717.
(25) Oosterhuis, W. T.; Lang, G. *Phys. Rev.* **1969**, *178*, 439.
(26) Griffith, J. S. *Mol. Phys.* **1971**, *21*, 135.
(27) Rhynard, D.; Lang, G.; Spartalian, K.; Yonetani, T. *J. Chem. Phys.* **1979**, *71*, 3715.
(28) Huynh, B. H.; Emptage, M. H.; Münck, E. *Biochem. Biophys. Acta* **1978**, *534*, 295.
(29) Dwivedi, A.; Toscano, W. A., Jr.; Debrunner, P. G. *Biochim. Biophys. Acta* **1979**, *576*, 502.
(30) Walker, F. A.; Huynh, B. H.; Scheidt, W. R.; Osvath, S. R. *J. Am. Chem. Soc.* **1986**, *108*, 5288.
(31) For α = 45°, the principal-axis systems of the $\tilde{g}$ and $\tilde{A}$ tensors remain aligned.[25]

A possible physical interpretation for the required rotation of the $\tilde{g}$ and $\tilde{A}$ tensor axes to achieve fits of the Mössbauer data is that the orientation of the $d\pi$ (d_{yz}, d_{xz}) orbitals does not correspond to the direction that is usually taken from the heme geometry. In other words, the planes of the two $d\pi$ orbitals are oriented between the Fe–N_p directions and perpendicular to the heme plane. If such an orientation of the $d\pi$ orbitals is indeed the correct one, it must result from the orientation of the axial nitrite ligands. The relatively high position of N-bound nitrite on the spectrochemical series suggests that it must be a good π-acceptor ligand. Effective π bonding between iron and nitrite requires a filled d orbital with lobes perpendicular to the nitrite plane. This condition would require that the d-orbital plane have an angle between 37 and 44° in the two complexes, close to the 45° values used in the fits.[32] (Cf. Figure S2 (supplementary material) for the relative orientations with respect to the heme). Finally, we note that in this analysis we have assumed that the principal magnetic direction (conventionally taken as z) corresponds to the heme normal in both the bis- and mono(nitro) complexes of this study. We have verified this assumption for the bis(nitro) complex by carrying out single-crystal EPR measurements.[33]

These preliminary EPR measurements have shown that g_z is approximately aligned along the heme normal and that g_x and g_y are in the heme plane in [K(18-C-6)(H_2O)][Fe(NO_2)$_2$-(TpivPP)]. Although we have not yet done any single-crystal EPR measurements on mixed pyridine or imidazole complexes, it is reasonable to assume that g_z is also aligned along the heme normal as it is in the bis(nitro), bis(pyridine),[22b] and bis(imidazole)[34] complexes from which the mixed-ligand complexes are constructed. It is also reasonable to predict that the mixed-ligand complexes would have g_y aligned along the projection of the plane of the nitro group, placing the empty π orbital of the nitro group where it can interact directly with the filled d_{xz} orbital of low-spin iron(III). We believe that the nitrite ion is a relatively weak σ donor and that the dominant interaction is between the filled $d\pi$ orbital of iron(III) and the unfilled π orbital of nitrite, i.e., M → L π back-bonding.

The g values of the two mixed-ligand complexes of this study, the bis(nitro) starting complex, and several other hexacoordinated low-spin iron(III) porphyrinates are reported in Table V. The Griffith model[26] for low-spin iron(III), as elaborated by Taylor[35] and Bohan,[36] and assuming the "typical" convention ($g_1 = g_z$ $g_2 = g_y$, and $g_3 = g_x$), leads to calculated values of the rhombicity (V/Δ)[12,37] that are larger than 0.67. The rhombicities of the mixed-ligand complexes are only slightly larger than 0.67, but that of the bis(nitro) complex is nearly double the limit expected for a "proper" axis system.[35] Although this might suggest a change in the direction of the principal magnetic axis for the bis(nitro) complex, we have verified that g_z is aligned close to the heme normal in this complex (vide supra). That the rhombicity is so large in these systems emphasizes the significant role played by the nitro ligand in orienting the orbital of the unpaired electron. The fact that the nitrite and pyridine (or imidazole) planes are approximately perpendicular would maximize π-acceptor interactions of the nitrite with the filled $d\pi$ orbital and π-donor interactions of the neutral ligand with the half-filled $d\pi$ orbital of Fe(III), assuming that the heterocyclic base is capable of π-donor interactions. We[39] and others[40] have previously presented evidence that suggests that imidazoles are stronger π donors than most pyridines. The length of the Fe–N(Ax) bonds in [Fe(NO_2)-(Py)(TpivPP)] and [Fe(NO_2)(HIm)(TpivPP)] are consistent with similar π donation from both neutral nitrogen ligands.

In an attempt to develop a consistent picture of the magnetic behavior of low-spin iron(III) porphyrinates, we have compared the nitrite–neutral ligand complexes of this study with other anion–neutral ligand species. Structural data and EPR parameters have been measured for the N-bound thiocyanate–pyridine,[21] azide–imidazole,[41] and cyanide–pyridine[20,22b] complexes of iron-(III) porphyrinates, as well as the unusual low-spin five-coordinate complex [Fe(TPP)(C_6H_5)].[42,43] The anions of this series span a large region of the spectrochemical series, $N_3^- < NCS^- < NO_2^- < C_6H_5^- < CN^-$, with azide considered to be a π donor, N-bound thiocyanate fairly neutral, nitrite a π acceptor, $C_6H_5^-$ a strong σ donor, and cyanide both a strong σ donor and π acceptor. For the N-bound thiocyanate–pyridine combination, we have been unable to obtain an EPR spectrum down to 5 K, save for a very weak feature in the region g = 2.87–2.93, similar in position to g_1 of the nitro–pyridine and nitro–imidazole complexes of the present study. Balch and co-workers[42] have reported the single feature observed in the EPR spectrum of the phenyl complex. It, like the cyanide–pyridine combination,[22b] is clearly of the "large g_{max}" type,[30] despite the presence of a planar axial ligand.[44] Thus for the thiocyanate–pyridine and phenyl complexes it is not possible to calculate the rhombicity and tetragonality, although some limits can be defined for the phenyl complex. For the others, however, we find that the tetragonality varies from 1.3 (cyanide–pyridine) to 2.9 (nitrite–imidazole). In the absence of reliable g values for an azide–pyridine complex, we have used the values obtained by Hori[41] for metmyoglobin azide. The rhombicity varies from 0.3 (cyanide–pyridine) to the very large value of 0.74 (nitrite–pyridine). Strouse and co-workers have discussed in detail the ambiguity in the sign of g_x and the product $g_xg_yg_z$ for [Fe(TPP)-(CN)(Py)]. However, independent of this ambiguity, the half-filled orbital is d_{yz}.[22b] While the exact definition of the EPR parameters for the phenyl complex awaits a single-crystal EPR investigation, the limits given in Table V are sufficient for the present discussion.[45] We see that the rhombicity is quite small for the phenyl complex, as it is for the cyanide–pyridine complex, despite the fact that in both cases there is one planar axial ligand. The most revealing difference in the calculated parameters for these mixed-ligand complexes, whose EPR spectra range in type from typical rhombic to nearly axial to "large g_{max}", is the degree of localization of the unpaired electron in the d_{yz} orbital, as measured by orbital-mixing coefficient a. For the typical rhombic and nearly axial types (nitrite–pyridine, nitrite–imidazole, azide–imidazole) the value of a^2 is 0.9 or greater (90% of the unpaired electron is in d_{yz}), while for the large g_{max} types (cyanide–pyridine, phenyl) the value of a^2 is less than 0.7 (68% or less of the unpaired electron of the phenyl complex is in d_{yz}; 59% for the cyanide–pyridine complex). It thus appears that a wide variety of orbital interaction types are able to stabilize a d_{yz} ground state for low-spin iron(III) porphyrinates, including strong π donors, strong σ donors, and strong π acceptors. The type of EPR spectra observed appear to be independent of whether the

(32) The observed[10] nitrite orientation angles in [K(18-C-6)(H_2O)][Fe-(NO_2)$_2$(TpivPP)] are 37 and 44° and in the mixed nitro–pyrimidine complex 37°. We have used a value of α = 45° in the fits because of the substantial computational simplicity. Qualitatively, an α value of ~40° would seem to yield still better fits to the experimental Mössbauer data in applied fields.
(33) Lloyd, S.; Huynh, B. H.; Nasri, H.; Scheidt, W. R. Work in Progress.
(34) Soltis, S. M.; Strouse, C. E. *J. Am. Chem. Soc.* **1988**, *110*, 2824.
(35) Taylor, C. P. S. *Biochim. Biophys. Acta* **1977**, *491*, 137.
(36) Bohan, T. *J. Magn. Reson.* **1977**, *26*, 109.
(37) Peisach, J.; Blumberg, W. E.; Adler, A. D. *Ann. N.Y. Acad. Sci.* **1973**, *206*, 310. Brautigan, B. L.; Feinberg, B. A.; Hoffmann, B. M.; Margoliash, E.; Peisach, J.; Blumberg, W. E. *J. Biol. Chem.* **1977**, *252*, 574.
(38) Huynh, B. H.; Emptage, M. H.; Münck, E. *Biochim. Biophys. Acta* **1978**, *534*, 295.
(39) Ramsey, B. G.; Walker, F. A. *J. Am. Chem. Soc.* **1974**, *96*, 3314.
(40) Ramsey, B. G. *J. Org. Chem.* **1979**, *44*, 2093. Johnson, C. R.; Shepherd, R. E. *Inorg. Chem.* **1983**, *22*, 3506.
(41) Hori, H. *Biochim. Biophys. Acta* **1971**, *251*, 227.
(42) Arasasingham, R. D.; Balch, A. L.; Hart, R. L.; Latos-Grazynski, L. *J. Am. Chem. Soc.*, in press. The structure of this complex has been reported previously.[43]
(43) Doppelt, P. *Inorg. Chem.* **1984**, *23*, 4009.
(44) Since the large g_{max} signal arises from a near degeneracy of the d_{xz} and d_{yz} orbitals, a nearly axially symmetric interaction with the axial ligand is required. Thus the phenyl group must be acting as a pure σ donor.
(45) The phenyl complex has a maximum possible g_y of 1.86 (for g_x = 0), leading to a minimum tetragonality of 1.6 and maximum rhombicity of 0.3 (Table V). The minimum possible value of g_y is less clearly defined, but if we assume that it is unreasonable for the tetragonality to be much above 5.0, then the minimum value of g_y is approximately 1.6, leading to a maximum g_x of 0.95 and a minimum rhombicity of 0.15 (Table V).

π-orbital interaction is donor or acceptor, but are quite sensitive to strong σ-donor interactions, to the point where large g_{max} EPR spectra can be observed even in the presence of a single planar ligand.

In summary, the electronic structures of bis(nitro) and mixed-axial-ligand mono(nitro) iron(III) porphyrinates have been examined by Mössbauer and EPR spectroscopies. The electronic structure is dominated by the strong π-acceptor character of N-bound nitrite, which can be deduced by the relatively large rhombicities (difference in energy of the d_{xz} and d_{yz} orbitals).

Acknowledgment. We thank the National Institutes of Health for support of this research through Grants GM-38401 (W.R.S.) and DK-31038 (F.A.W.) and the National Science Foundation through Grant DMB 9001530 (B.H.H.). We also thank Martin Safo for synthesizing a sample of [Fe(TPP)(NCS)(Py)] for EPR measurements.

Supplementary Material Available: Tables SI–SVIII, giving complete crystallographic details, anisotropic thermal parameters, fixed hydrogen atom positions, and complete bond distances and angles for [Fe(NO_2)(Py)(TpivPP)] and [Fe(NO_2)(HIm)(TpivPP)], Figure S1, showing a mean plane diagram for [Fe(NO_2)(HIm)(TpivPP)], and Figures S2 and S3, showing nitrite, imidazole, and pyridine orientations (16 pages); listings of observed and calculated structure amplitudes (×10) for both compounds (37 pages). Ordering information is given on any current masthead page.

Contribution from the Department of Chemistry, Queen Mary and Westfield College, Mile End Road, London E1 4NS, England, Dipartimento di Chimica Inorganica, Chimica Fisica e Chimica dei Materiali, Universita di Torino, Via P. Giuria 7, 10125 Torino, Italy, and Department of Inorganic Chemistry, University of Oxford, South Parks Road, Oxford OX1 3QR, England

Use of Solid-State ^{13}C NMR Spectroscopy to Quantify the Degree of Asymmetry of Bonding for Semibridging CO Groups in Iron Carbonyl Complexes

Geoffrey E. Hawkes,*[1a] Keith D. Sales,[1a] Silvio Aime,[1b] Roberto Gobetto,[1b] and Lu-Yun Lian[1c,d]

Received August 9, 1990

The solid-state ^{13}C NMR spectra of some substituted iron carbonyl complexes have been analyzed to give values for the carbonyl carbon chemical shift tensor components. It is shown that the lowest frequency tensor component and the chemical shift anisotropy correlate with the degree of bonding asymmetry in double-bridging carbonyl groups, whereas the ^{13}C isotropic chemical shift does not correlate. The correlations are proposed to form the basis for a method of estimating iron–carbon bond lengths for μ_2-CO groups in this type of complex.

Introduction

Infrared (IR) spectroscopy is widely used in the study of metallocarbonyl complexes; in particular the C–O bond stretching frequency may be directly correlated with the metal–carbon bonding. As described by Cotton and Wilkinson,[2] terminal carbonyl groups (M–CO) in neutral molecules generally absorb in the region 1850–2125 cm^{-1}, while bridging CO groups absorb in the region 1700–1860 cm^{-1}. Isotropic ^{13}C shieldings measured from either solution or solid-state NMR spectra may also be diagnostic of the bonding. These observations are typified by data for $Fe_2(CO)_4(\eta^5\text{-}C_5H_5)_2$ (I), which in octane solution has IR absorptions at 1794 cm^{-1} due to symmetric double bridging CO groups and at 1961 and 2005 cm^{-1} due to terminal CO groups[3] and has solution ^{13}C chemical shifts at 273.2 (bridging CO) and 210.2 ppm (terminal CO).[4] For *semibridging* CO groups which are shared unequally between two iron atoms (Fe_b---CO–Fe_a) the frequencies of the IR absorptions may not be so readily interpreted in terms of degree of bridging character or asymmetry. It is known that the isotropic ^{13}C chemical shifts for asymmetric briding CO groups may occur between the extremes exhibited by the bridging and terminal groups of I; for example the asymmetric bridging CO group in $Fe_3(CO)_8(PhC_2Ph)_2$ has its ^{13}C chemical shift at 253.7 ppm.[5] However the symmetric bridging CO group of $Fe_2(CO)_9$ has its ^{13}C resonance at 235.9 ppm.[6] Clearly, the exact value for the isotropic ^{13}C shift does not reflect the *degree* of symmetry in the bridging. The present study is concerned with the analysis of the slow magic angle spinning (MAS) solid-state ^{13}C spectra to provide the principal components of the chemical shift tensor (δ_{11}, δ_{22}, δ_{33}) and the chemical shift anisotropy ($\Delta\delta$, see below) as well as the ^{13}C isotropic shift (δ_{iso}), and the investigation of possible correlations between these additional parameters and the degree of bridging asymmetry. Recently, Carty et al.[7] reported correlations between the ^{31}P chemical shift tensor components and M–P–M (M = Fe, Ru, Os) bond angles in a series of phosphido-bridged complexes.

Experimental Section

Materials. All carbonyl complexes employed in this study were ^{13}CO enriched. *cis* and *trans*-$Fe_2(CO)_4(\eta^5\text{-}C_5H_5)_2$ (I) were obtained as a commercial mixture (Strem Chemicals), and ^{13}C enrichment was performed on the commercial product by heating at 60 °C (*n*-hexane as solvent) under ca. 1 atm 99% ^{13}CO gas for 2 days in sealed vials. The enrichment achieved was ca. 35–40%. The cis isomer was obtained by crystallization from a dichloromethane solution, and the trans isomer from an *n*-heptane solution. $Fe_2(CO)_6PhC_2Ph$ (II), the black isomer of $Fe_3(CO)_8(PhC_2Ph)_2$ (III), and $Fe_3(CO)_{11}PPh_3$ (IV) were all prepared from ^{13}C-enriched $Fe_3(CO)_{12}$ by the methods of Hubel and Braye,[8] Dodge and Schomaker,[9] and Angelici and Siefert,[10] respectively. The phosphine complex (IV) was purified by crystallization from chloroform/pentane at −20 °C. ^{13}C-enriched $Fe_2(CO)_9$ (V) was prepared by irradiation of a solution of ^{13}C-enriched iron pentacarbonyl in acetic acid using a 125-W high-pressure mercury lamp for 24 h. The enrichment of the iron pentacarbonyl (ca. 40% ^{13}C) was achieved by using the procedure of Shore and co-workers[11] with $NaBH_4$ as exchange promoter. The preparation of ^{13}C-enriched $Fe_3(CO)_{12}$ (VI) has been described previously.[12] Levels of ^{13}C enrichment were estimated by using mass spectrometry.

NMR Spectra. Solid-state ^{13}C spectra were recorded by using the cross polarization/magic angle spinning (CP/MAS) technique at 50.3 MHz (Bruker CXP-200) and 75.5 MHz (Bruker MSL-300) as previously described.[12,13] Samples (typically 100–200 mg) were contained

(1) (a) Queen Mary and Westfield College. (b) Universita di Torino. (c) University of Oxford. (d) Present address: Biological NMR Centre, Department of Biochemistry, University of Leicester, University Rd., Leicester LE1 7RH, U.K.
(2) Cotton, F. A.; Wilkinson, G. *Advanced Inorganic Chemistry*, 5th ed; Wiley: New York, 1988; p 1034.
(3) Cotton, F. A.; Yagupsky, G. *Inorg. Chem.* **1967**, *6*, 15–20.
(4) Gansow, O. A.; Burke, A. R.; Vernon, W. D. *J. Am. Chem. Soc.* **1972**, *94*, 2550–2552. Gansow, O. A.; Burke, A. R.; Vernon, W. D. *Ibid.* **1976**, *98*, 5817–5826.
(5) Hickey, J. P.; Wilkinson, J. R.; Todd, L. J. *J. Organomet. Chem.* **1975**, *99*, 281–286. Aime, S.; Milone, L.; Sappa, E. *Inorg. Chim. Acta* **1976**, *16*, L7–L8.
(6) Dorn, H. C.; Hanson, B. E.; Motell, E. *J. Organomet. Chem.* **1982**, *224*, 181–187.
(7) Carty, A. J.; Fyfe, C. A.; Lettinga, M.; Johnson, S.; Randall, L. H. *Inorg. Chem.* **1989**, *28*, 4120–4124.
(8) Hubel, W.; Braye, E. H. *J. Inorg. Nucl. Chem.* **1959**, *10*, 250–268.
(9) Dodge, R. P.; Schomaker, V. *J. Organomet. Chem.* **1965**, *3*, 274–284.
(10) Angelici, R. J.; Siefert, E. E. *Inorg. Chem.* **1966**, *5*, 1457–1459.
(11) Bricker, J. C.; Payne, M. W.; Shore, S. G. *Organometallics* **1987**, *6*, 2545–2547.
(12) Hawkes, G. E.; Sales, K. D.; Lian, L. Y.; Gobetto, R. *Proc. R. Soc. London A* **1989**, *424*, 93–111.

0020-1669/91/1330-1489$02.50/0